J Fluoresc (2011) 21:1009–1013
DOI 10.1007/s10895-010-0776-0

SHORT COMMUNICATION

Locating of Nucleic Acid Intercalators in Yeast Cells by Image Analysis Combined Fluorescence Microscopy

Evgeny O. Puchkov · Millicent McCarren

Received: 21 September 2010 / Accepted: 16 November 2010 / Published online: 3 December 2010

Abstract Intracellular distribution in the intact (not fixed) *Saccharomyces cerevisiae* cells of the nucleic acid intercalators (NAI) was studied using fluorescence microscopy combined with computer image analysis (ImageJ software, NIH, USA). Three NAI—the anthracycline anticancer drug doxorubicin (DR) along with the nucleic acid dyes ethidium (E) and 4′,6-diamidino-2-phenylindole (DAPI)—were used. Staining pattern and ImageJ quantitative analysis data provided evidence that all three NAI were located in the nuclei and in the mitochondria. DR and E, in contrast to DAPI, may be bound to not only DNA, but to the mitochondrial membranes as well. Experiments on the combined application of DR+DAPI and E+DAPI have shown potential competition of DAPI with DR and E for binding sites in the nuclear and mitochondrial DNA. With the approach presented herein, the yeast cells of *S. cerevisiae* can be used as a model for locating intracellular sites of the fluorescing nucleic acid intercalators. This model may be of help in designing new DNA-targeted drugs and in preliminary studies of their interaction with eukaryotic cells.

Keywords Fluorescence microscopy · Image analysis · Yeast · Anticancer drug · Intercalator

E. O. Puchkov (✉)
G.K.Skryabin Institute of Biochemistry and Physiology
of Microorganisms, RAS,
Institutskaya Str., 5,
Pushchino 142290, Russia
e-mail: puchkov@ibpm.pushchino.ru

M. McCarren
University of Pittsburgh,
Pittsburgh, PA, USA

Introduction

The nucleic acid intercalators (NAI) are chemically diverse positively charged amphiphilic polyaromatic molecules containing fused rings [1]. Many of them, if not all, are fluorochromes. Some NAI are well known as nucleic acid stains (dyes) or probes [2]. However, interaction of NAI with nucleic acids is not specific. They can bind to various macromolecular complexes as well, as it was shown with isolated polymers [3, 4], biological and artificial membranes [5, 6], and living cells [7, 8]. These interactions may play a role in the overall effects of the NAI upon living cells.

Of special interest are NAI with anticancer activity. The main problems with clinical application of these drugs are multidrug resistance of some cancer cells and side/toxic effects [9]. For better understanding of both therapeutic and side/toxic effects of drugs, their intracellular location/distribution needs to be elucidated. This can be done by single live cell studies with mammalian cell lines as models [8, 10]. These models are expensive, tiresome and restricted in potential molecular or genetic manipulations.

Yeast cells of *Saccharomyces cerevisiae* are broadly used as a model system for studies of eukaryotic cells since many of the basic cellular properties between yeast and humans are highly conserved. This is also due to the availability of the DNA sequence of the complete genome and biochemical data, convenience for molecular manipulations and the ease of handling [11]. The yeast cells are shown to be a good model in many areas of cancer research [12] and for new drug discovery [13]. However, yeasts were not used as a model for intracellular location/distribution of drugs as of yet.

The aim of this study was to test if intact (not fixed) yeast cells of *S. cerevisiae* can be used as a model for

locating intracellular sites/targets of the NAI. To this end, intracellular distributions of three fluorescing NAI—the anthracycline anticancer drug doxorubicin (DR) (trade name adriamycin; also known as hydroxydaunorubicin) along with nucleic acid dyes ethidium (E) and 4′,6-diamidino-2-phenylindole (DAPI), were investigated using fluorescence microscopy combined with computer image analysis.

Materials and Methods

Culture and Growth Conditions

A type strain of *S. cerevisiae* VKM Y-2549 from the All-Russian Collection of Microorganisms was used throughout the work. The culture was maintained on slants of agarized (1.5%) wort (4%) medium at 4 °C. The cells from the slants were seeded into 20 ml of a liquid medium containing 0.63% Yeast Nitrogen Base (Becton Dickinson Microbiology Systems, USA) and 2% glucose in conic flasks. After incubating at static conditions at 23±1 °C for 18–24 h, 2 ml of this culture was used as inoculum to seed 20 ml of the fresh medium. This culture was incubated at the same conditions for another 18–24 h and used as a source of the cells for experiments. Concentration of the cells was assessed by photometry after calibration using Goryaev chamber for cell counting as described in [14]. Concentration of the cells in the cultures used was $1.5–2.0\times10^8$ cells/ml.

Preparation of Specimens for Microscopy

Cells were concentrated by centrifugation up to approx. 5×10^8 cells/ml and samples supplemented with intercalators were prepared. The following final concentrations of the NAI were used: 4,6-diamidino-2-phenylindole, dilactate (DAPI) (Sigma, USA)—3 μM; ethidium bromide (E) (3,8-diamino-5-ethyl-6-phenylphenanthridinium bromide) (Serva, Germany)—10 μM and doxorubicin (DR) (Ferane-Bryncalov, Russia)—10 μM. After incubating for various time intervals at 20–23 °C, 4 μl aliquots of a cell suspension were placed onto specimen slides, covered with a cover glass, and sealed with nail polish at the periphery of the cover glass to prevent evaporation. Observations were started approx. 30 min after sealing, when most cells had stuck to the slide's glass.

Fluorescence Microscopy and Color Digital Photography

Fluoresce microscopy and color digital photography were carried out on a ML-2B fluorescence microscope (LOMO, Russia) as described in [15] with some modifications. Two filter sets were used for fluorescence observations and photography. 1) A UFS-6 filter in the fluorescence excitation path and a ZhS-3 filter in the fluorescence emission path were installed, that gave $\lambda_{ex}/\lambda_{em}$ – 360 nm/>400 nm. 2) A SS-15 filter in the fluorescence excitation path and a ZhS-18 filter in the fluorescence emission path were installed, that gave $\lambda_{ex}/\lambda_{em}$ – 430 nm/>520 nm. The first filter set is most suitable for the visual observations of DAPI fluorescence in nucleic acids [2, 16]. The second set is convenient for the visual observations of DR [17] and E [18] fluorescence. However, in principal, both filter sets can be used for observations and fluorescence measurements of all three NAI. In the light transmission mode of operation, a combination of glass filters with transmittance λ_{max} near 520 nm in front of an object and a ZhS-3 filter (transmittance λ >400 nm) behind it were installed. For the publication, the color images were transformed into the 8-bit gray ones.

Computer Image Analysis

The color digital images of the fluorescing cells were processed by the Adobe Photoshop, v. 8.0 (Adobe Systems Inc., USA) and analyzed by the ImageJ 1.42 (National Institute of Health, USA, http://rsb.info.nih.gov/ij) software. Red, green and blue components of the fluorescence intensity were quantitatively assessed in the selected regions of interest (ROI "Oval Selection") of the images using "Analyze" plugin ("Measure RGB" option). The obtained data were in the arbitrary units of the 8-bit gray scale (0–256 units). Fluorescence intensity Red/Green and Blue/Green ratios were presented as means with standard deviations.

Results and Discussion

Visual observations have shown that all the cells were well stained by DAPI within 2 h of incubation. Incubation for at least 20 h was required to make all the cells to be stained by DR and E. There was heterogeneity of the cell populations in the stainability by DR and E. Some cells were brightly fluorescent, while glowing of the others was less pronounced. The observed difference in the stainability may be a reflection of specific permeability of the individual cells for the NAI. The permeability is a combination of at least two factors. The first is the diffusion barrier properties of the cell wall and of the cytoplasmic membrane [19]. The second may be related to the presence of drug export permeases [20] which provide for the energy dependent excretion of cationic organic molecules out of the cells. So, the amount of permeated dyes may depend on the

energetic status of the cells. One more thing should be kept in mind regarding staining by the NAI. Upon binding to the nucleic acids, fluorescence of DR may decrease [21], in contrast to increasing fluorescence of DAPI [2] and E [18].

In the cells with DNA stained by DAPI, there were clearly visible fluorescing blue spots of the nuclei and small dots of the mitochondria (Fig. 1b) [16]. As compared to DAPI (Fig. 1b), intracellular fluorescence distribution of DR (Fig. 1d) and E (not shown) had not the clear "spot and dot" appearance. Although nuclear region could be distinguished, even distribution of the DR and E glowing was observed in the regions where mitochondria should be located. Application of DAPI with DR visualized location of the nuclear and of the mitochondrial DNA (Fig. 1f). Similar picture was observed with E (not shown). However, visual analysis could not answer the question whether DR and E were located in the sites of the DAPI-stainable DNA.

It follows from the fluorescence spectra comparison that DR [17] and E [18] fluorescence has pronounced red component while in the DAPI glowing the main component is blue-green light [2, 16]. To investigate potential location of DR and E in the nuclei and in the mitochondria marked by DAPI, distribution of the red, green and blue components of the fluorescence in these regions was assessed quantitatively using image analysis.

In Part 1 of the Table 1, the data of the experiments when the cells were treated with a single NAI are presented. Since there were no clearly distinguished mitochondrial "dots" in the images of the cells treated by DR (see Fig. 1d) and E alone, fluorescence intensity was assessed in the areas corresponding to the potential mitochondrial location (Fig. 1b). Part 2 of the Table 1 contains data of the combined applications of DAPI and DR or E.

The data of Table 1 (Part 1) indicate that, as it was expected, DAPI fluorescence had markedly higher the B/G ratio than the R/G ratio (columns 1 and 2) and it was vice versa for fluorescence of DR (columns 3 and 4) and of E (columns 5 and 6). Both R/G and B/G ratios for DAPI (columns 1, 2) and for E (columns 5, 6) were almost identical in the nuclei and in the mitochondrial region. On the contrary, DR fluorescence had appreciably higher the R/G ratio in the nuclei than in the mitochondrial region (columns 3, 4). These data indicated that fluorescence spectra of at least a fraction of DR molecules bond in the nuclei had more expressed red component than those in the mitochondrial region.

Interaction of DR with nucleic acids is known to increase the "red" maximum in its fluorescence spectrum [17]. So, the less expression of the red fluorescence in the mitochondria may be explained assuming that, along with binding to DNA, some molecules of DR are bound to the membranes. Binding to the membranes may also be a

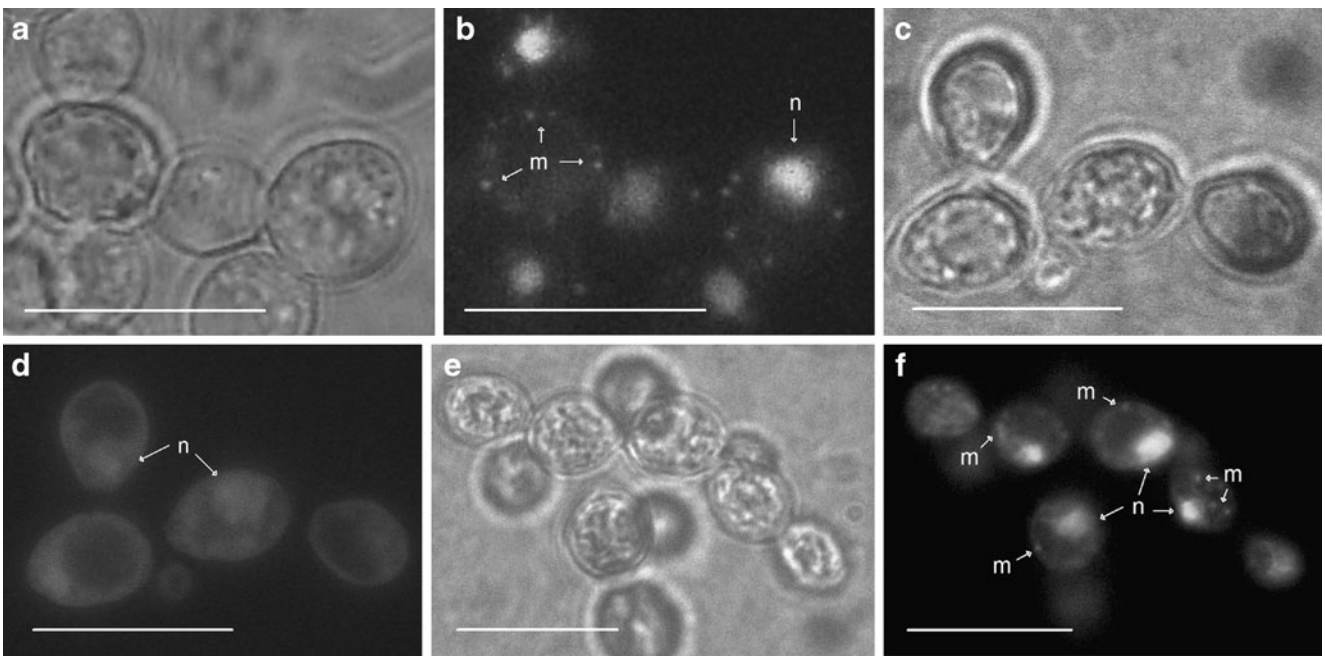

Fig. 1 The cells of *Saccharomyces cerevisiae* VKM Y-2549 stained by DAPI (**a**, **b**), Doxorubicin (**c**, **d**) and combination of DAPI and Doxorubicin (**e**, **f**). **a**, **c** and **e**, transmission mode. **b**, **d** and **f**, fluorescence mode ($\lambda_{ex}/\lambda_{em}$ – 360 nm/>400 nm). n, nuclei; m, mitochondria. Bars = 10 μm

Table 1 Ratios of the red (R), green (G), and blue (B) components of the fluorescence intensity of DAPI, DR, and E in the nuclei and mitochondria of the *S. cerevisiae* cells[a]

Part 1	DAPI		DR		E		Part 2	(DAPI + DR)[c]		(DAPI + E)[c]		(DR + DAPI)[d]		(E + DAPI)[d]	
	1	2	3	4	5	6		7	8	9	10	11	12	13	14
	Nuclei ($n=7$)[b]	Mitochondria ($n=10$)	Nuclei ($n=8$)	"Mitochondrial region" ($n=11$)	Nuclei ($n=8$)	"Mitochondrial region" ($n=16$)		Nuclei ($n=8$)	Mitochondria ($n=15$)	Nuclei ($n=6$)	Mitochondria ($n=12$)	Nuclei ($n=6$)	Mitochondria ($n=14$)	Nuclei ($n=9$)	Mitochondria ($n=11$)
R/G ± sd	0,02±0,02	0,02±0,01	0,95±0,05	0,71±0,05	4,3±0,3	4,5±0,1	R/G ± sd	0,22±0,06	0,10±0,03	0,98±0,11	1,28±0,08	0,47±0,07	0,27±0,04	0,84±0,1	0,9±0,1
B/G ± sd	0,86±0,04	0,88±0,02	0,37±0,03	0.4±0,07	0,04±0,01	0,06±0,02	B/G ± sd	0,90±0,06	0.84±0,05	0,96±0,08	0,7±0,2	0,9±0,1	0,89±0,07	0,88±0,04	0,78±0,1

[a] Fluorescence microscopy and digital photography were carried out with a filter set that gave λex/λem – 360 nm/>400 nm. Fluorescence intensities in the corresponding regions of the images were measured using ImageJ software as described in Materials and Methods

[b] n – The number of regions, where fluorescence intensities were measured

[c] The cells were examined after incubating for 20 h with the combination of DAPI and DR or E added simultaneously

[d] Upon incubating of the cells with DR or E for 20 h, DAPI was added, and the samples were examined after another 6 h of incubation

plausible reason for visible even fluorescence distribution in the mitochondrial region in the cells stained by DR (Fig. 1d) as compared to "dot"-like staining of the mitochondrial DNA by DAPI (Fig. 1b). A similar picture was observed for E fluorescence in this region (not shown). There may be at least two binding sites for DR and E in the mitochondria: DNA and the membranes. Ability of E to interact with the membranes of the isolated mitochondria was demonstrated by others [5]. Potential ability of DR to interact with biomembranes was shown on artificial membranes [6].

Upon combined addition of DR+DAPI simultaneously, in both the nuclei and in the mitochondria, the R/G fluorescence ratio was higher (columns 7, 8) as compared to the application of DAPI alone (columns 1, 2), but it was lower as compared to exposing the cells to DR only (columns 3, 4). If the cells were first incubated with DR, and DAPI was added later, the R/G ratio in the nuclei was higher (columns 11, 12) than in case of simultaneous addition of the NAI (columns 7, 8), but still lower than after the addition of DR alone (columns 3, 4). Similar results were obtained for the pair E+DAPI with the difference that the order of the NAI addition did not significantly influence the final result (columns 9, 10 and 13, 14). At the same experimental conditions, there were no appreciable changes in the B/G ratio.

Appearance of the red fluorescence component in the regions of DAPI stained DNA upon combined application of DAPI with DR and E is an indication of a colocalization of DAPI with DR and E in the nuclei and in the mitochondria. In the sites of the colocalization of DR and E with DAPI, the red component of their fluorescence was less as compared to the application of DR and E alone. These data can be interpreted as a competition of DAPI with DR and E for the same DNA binding sites. It should be mentioned here that, although NAI can intercalate between base pairs, they may also be bound to some other parts of DNA, e.g. in the minor groove [2, 17, 18, 22]. We found no data in the literature on DAPI competition with DR and E for binding to isolated DNA. The detailed mechanism of the competition of DAPI, DR and E for binding sites in DNA is not known as of yet.

In conclusion, the results of this study demonstrated that the intact (not fixed) yeast cells of *S. cerevisiae* can be used as a model for locating intracellular sites/targets of the fluorescing nucleic acid intercalators by fluorescence microscopy combined with computer image analysis. Of special interest may be the use of this model for studies of the NAI permeation and intracellular distribution dynamics. In general, the model and the approach presented herein may be of help in designing of new DNA-targeted drugs and in preliminary studies of their interaction with eukaryotic cells.

References

1. Denny WA (2003) In: Demeunynck M, Bailly C, Wilson WD (eds) DNA and RNA binders: from small molecules to drugs, vol 2. Wiley-VCH Verlag GmbH & Co. KGaA, Weinheim, pp 482–502
2. Haugland RP (1996) Handbook of fluorescent probes and research chemicals, 6th edn. Molecular Probes, Eugene, pp 144–152
3. Kido N, Ohta M, Kato N (1990) Detection of lipopolysaccharide by ethidium bromide staining after sodium dodecyl sulfate polyacrylamide gel electrophoresis. J Bacteriol 172(3):1145–1147
4. Smith SA, Morrissey JH (2007) Sensitive fluorescence detection of polyphosphate in polyacrylamide gels using 4, 6-diamidino-2-phenylindol. Electrophoresis 28(19):3461–3465
5. Gitler C, Rubalcava B, Caswell A (1969) Fluorescence changes of ethidium bromide on binding to erythrocyte and mitochondrial membranes. Biochim Biophys Acta 193(2):479–481
6. Gallois L, Fiallo M, Laigle A et al (1996) The overall partitioning of anthracyclines into phosphatidyl-containing model membranes depends neither on the drug charge nor the presence of anionic phospholipids. Eur J Biochem 241(3):879–887
7. Puchkov EO, Yurkova TV, Golubev WI (1998) Effects of Cryptococcus humicola killer toxin upon Cryptococcus terreus envelope: combined fluorometric and microscopic studies. Biochim Biophys Acta 1381(1):61–67
8. Willingham MC, Cornwell MM, Cardarelli CO et al (1986) Single cell analysis of daunomycin uptake and efflux in multidrug-resistant and -sensitive KB cells: effects of verapamil and other drugs. Cancer Res 46(11):5941–5946
9. Martínez R, Chacón-García L (2005) The search of DNA-intercalators as antitumoral drugs: what it worked and what did not work. Curr Med Chem 12(2):127–151
10. Gigli M, Doglia SM, Millot JM et al (1988) Quantitative study of doxorubicin in living cell nuclei by microspectrofluorometry. Biochim Biophys Acta 950(1):13–20
11. Botstein D, Chervitz SA, Cherry JM (1997) Yeast as a model organism. Science 277(5330):1259–1260
12. Nitiss JL, Heitman J (eds) (2007) Yeast as tool in cancer research. Springer, Dotdrecht
13. Mager WH, Winderickx J (2005) Yeast as a model for medical and medicinal research. Trends Pharmacol Sci 26 (5):265–273
14. Puchkov EO (2009) Application of an automated colony counter for evaluation of the viability of a yeast culture. Microbiology 78 (4):502–509
15. Puchkov EO (2010) Brownian motion of polyphosphate complexes in yeast vacuoles: characterization by fluorescence microscopy with image analysis. Yeast 27(6):309–315
16. Williamson DH, Fennell DJ (1979) Visualization of yeast mitochondrial DNA with the fluorescent stain “DAPI”. Methods Enzymol 56:728–733
17. Angeloni L, Smulevich G, Marzocchi MP (1982) Absorption, fluorescence and resonance Raman spectra of adriamycin and its complex with DNA. Spectrochim Acta, Part A: Mol Spectrosc 38 (2):213–217
18. Le Pecq JB, Paoletti C (1967) A fluorescent complex between ethidium bromide and nucleic acids: physical–chemical characterization. J Mol Biol 27(1):87–106
19. Klis FM, Mol P, Hellingwerf K, Brul S (2002) Dynamics of cell wall structure in Saccharomyces cerevisiae. FEMS Microbiol Rev 26(3):239–256
20. Rogers B, Decottignies A, Kolaczkowski M et al (2001) The pleitropic drug ABC transporters from Saccharomyces cerevisiae. J Mol Microbiol Biotechnol 3(2):207–214
21. Manfait M, Alix AJP, Jeannesson P et al (1982) Interaction of adriamycin with DNA as studied by resonance Raman spectroscopy. Nucleic Acids Res 10(12):3803–3816
22. Trotta E, D’Ambrosio E, Ravagnan G et al (1995) Evidence for DAPI intercalation in CG sites of DNA oligomer $[d(CGACGTCG)]_2$: a ^1H NMR study. Nucleic Acids Res 23(8):1333–1340